Identification of Critical Neutron-Rich Sn Isotopes in Rapid Neutron-Capture Process

Melvin Storbacka
melvin@storbacka.com

under the direction of
Assoc. Prof. Chong Qi
Department of Physics
KTH Royal Institute of Technology

Research Academy for Young Scientists
July 13, 2022

Abstract

About half of all elements heavier than iron-56 can be attributed to the rapid neutron-capture process, or the *r-process*. While the underlying processes are understood, there are still great uncertainties regarding where the r-process takes place and what site is most important for creating r-process elements. This study examined the importance of the masses of Sn-isotopes, with atomic mass numbers between $A = 146$ and $A = 166$, on the final elemental abundance of the r-process in different simulated environments. The initial temperature and mass density were varied to find the environment that depended most strongly on the Sn-isotope masses. Furthermore, the importance of individual isotope masses was tested in the most sensitive environment, by individually varying the masses of the Sn-isotopes. The results indicate that certain environments, where more highly neutron-rich nuclei are created, are more sensitive to the individual properties of heavy Sn-isotopes. The results also suggest that some isotopes may have much larger importance in the final abundance of the r-process. This provides a clue as to what isotopes are most important to measure experimentally as technology advances, which may improve the understanding of the r-process and potentially provide an answer to what the most important r-process site is.

Acknowledgements

I want to give my heartfelt thanks to Associate Professor Chong Qi for his guidance, insight and unwavering enthusiasm throughout our two weeks together. I am also grateful to Alexandra Arnmark for her insightful comments and discussions. Additionally, I want to express my gratitude towards Viktor Sundström, Felix Steinberger Eriksson, Ambjörn Joki, Arman Aspromonti and Tuva Källberg for their great feedback and advice. I would also like to thank Rays — for excellence and their collaborative partners Beijerstiftelsen, AstraZeneca and Olle Engkvists Stiftelse for giving me this incredible opportunity.

Contents

1 Introduction

One of the most important, yet poorly understood processes responsible for the creation of the elements in the universe is the r-process. The r-process, or *rapid neutron-capture process*, is a process in which elements become heavier by rapidly absorbing, or capturing, neutrons. While the synthesis of lighter elements, mainly hydrogen (H) and helium (He), has been well understood for a long time, there is still a lot of uncertainty regarding the synthesis of elements heavier than the iron isotope iron-56 (^{56}Fe). Understanding the underlying processes of the creation of these elements does not only provide insightful clues to aid the understanding of physics in general but develops the understanding of the history of the Milky Way and the solar system. This section covers the necessary theoretical background, the simulation code that was used, and explains the aim of this study.

1.1 Theory

The creation of elements heavier than iron-56, specifically through the r-process, is an active area of research [1, 2, 3, 4], incorporating both nuclear and astrophysical research. In this section, a brief summary of nucleosynthesis is provided. Furthermore, the relevant processes in the r-process are presented. Lastly, the limitations of the current knowledge regarding the r-process from an astrophysical as well as a nuclear perspective are explained.

1.1.1 Background

It has long been understood that the synthesis of light elements occurred in the first few minutes following the Big Bang [5], through a process called the *Big Bang Nucleosynthesis* (BBN) [6]. This process is very well understood, as it is comparatively easy to simulate, and the properties of involved elements can be measured experimentally [7]. The BBN started when the universe had existed for only a few tenths of a second [8]. During BBN, a

plethora of nuclear reactions were taking place, as atomic nuclei formed from the protons and neutrons available [9]. Through fusion of different nuclei, hydrogen, helium, lithium and beryllium were formed in different amounts. After approximately 20 minutes, the universe had expanded and cooled to the point that BBN reactions ceased [8]. Because the BBN occurred during a short time frame, hydrogen was most abundant when the BBN stopped, followed by helium [9]. The high *abundances*, or number of nuclei, of hydrogen and helium predicted by the BBN theory agree well with observations [10], making the BBN theory a widely accepted theory.

A few hundred million years after the Big Bang, the first stars began to form [11]. Inside these stars, energy is released mainly through fusion, which is when two nuclei combine into one while releasing energy [12]. The main fusion processes combine hydrogen nuclei to form helium. Helium nuclei are also combined to form heavier nuclei, such as carbon and oxygen [12]. However, fusion does not create elements heavier than iron-56, as this is the most stable nucleus. Simultaneously, a process called the *s-process*, or the slow neutron-capture process, takes place. In the s-process, nuclei capture free neutrons to gain mass, and subsequently undergo β^--decay to become a different element [13]. The s-process can create elements much heavier than iron-56, but does not explain the total abundance of these heavier nuclei.

1.1.2 r-process

The creation of about half of all elements heavier than iron-56 can be attributed to the rapid neutron-capture process, which is usually called the *r-process* [1]. This is a process in which atomic nuclei, called *seed nuclei*, capture neutrons and become heavier, similarly to in the s-process. In the reaction, a seed nucleus captures a neutron and releases energy in the form of electromagnetic radiation. This nuclear reaction can be written as (n, γ), or

$$ {}^{A}_{Z}X + n \longrightarrow {}^{A+1}_{Z}X + \gamma, \tag{1} $$

where X is the chemical symbol of the element, Z is the atomic number, A is the atomic mass number, n is a neutron, and γ is the emitted electromagnetic radiation [14]. The atomic mass number A is equal to $Z + N$, where N is the number of neutrons in the nuclei.

When a nucleus is unstable due to a great excess of neutrons in the nucleus, it may undergo a process known as β^--decay [15]. During this process, a neutron in the nucleus converts to a proton by emitting an electron, e^-, and an electron anti-neutrino, $\overline{\nu}_e$. The β^--decay process can be expressed as the nuclear reaction

$$ {}^{A}_{Z}X \longrightarrow {}^{A}_{Z+1}Y + e^- + \overline{\nu}_e, \tag{2} $$

from which it is evident that the element changes during β^--decay, though the atomic mass number, A, remains constant [14]. Throughout the rest of this paper, any mention of β-decay refers to β^--decay, specifically.

During the r-process, the rate of incoming neutrons, called the *neutron flux*, is very high in comparison to the s-process [2]. While the s-process occurs during the normal life of a star when the neutron flux is relatively low, the r-process occurs in an explosive environment with very high neutron flux [2]. If a time scale, τ_n, is the approximate time required for an additional neutron to be absorbed, and τ_β is the time scale for β-decay to occur, it is true for the r-process that $\tau_n \ll \tau_\beta$ [14]. The time scale τ_n depends strongly on the environmental neutron flux, while τ_β is determined by the composition of the nucleus, often called the *nuclear species* [14]. This means that as long as there is sufficient neutron flux, the neutron capture process will proceed much faster than the β-decay, and dominate the r-process mechanism. For comparison, the opposite is true in the s-process; As $\tau_n \gg \tau_\beta$, the process evolves very slowly, and any neutron capture is immediately followed by β-decay [14].

While nuclei absorb neutrons by neutron capture, there will be an opposite reaction, known as *photodisintegration*, caused by γ-rays emitted by the high-temperature matter

in which the r-process should take place. In the reaction, the γ-rays are absorbed by a nucleus, which causes it to decay by emitting a neutron. This nuclear reaction can be expressed as

$$ {}^{\mathrm{A}}_{\mathrm{Z}}\mathrm{X} + \gamma \longrightarrow {}^{\mathrm{A}-1}_{\mathrm{Z}}\mathrm{X} + n, \tag{3} $$

and is also written as (γ, n) [14].

With sufficient neutron flux, a given element will capture neutrons, so that different isotopes are created along an *isotope chain*. As more neutrons are absorbed in the (n, γ) reaction, the nucleus generally becomes more unstable. If a nucleus created in the process is very unstable, it is more likely to undergo (γ, n) photodisintegration. Because of this, a $(n, \gamma) \rightleftharpoons (\gamma, n)$ equilibrium can occur [2]. A $(n, \gamma) \rightleftharpoons (\gamma, n)$ equilibrium along an isotope chain is shown in Figure 1. It should also be noted that there exists an upper limit to

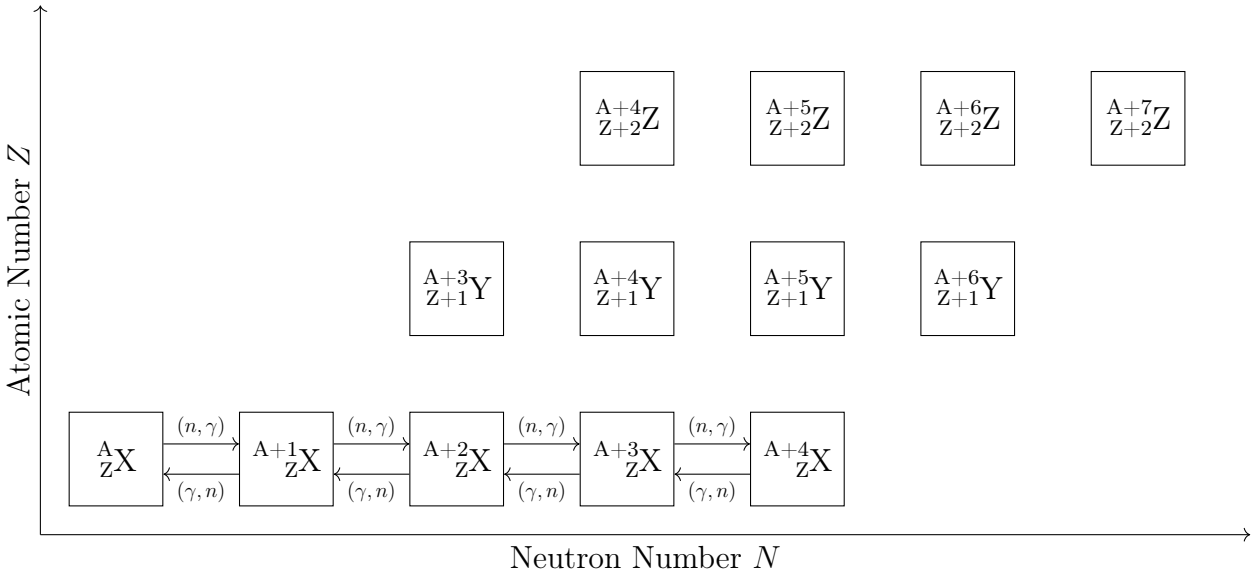

Figure 1: Neutron capture-photodisintegration equilibrium in an isotope chain of atomic number Z, shown in the NZ-plane. Neutron capture, (n, γ), moves the nucleus to the right in the N-direction, while photodisintegration, (γ, n), moves the nucleus to the left in the N-direction.

the number of neutrons a given element can contain, known as the *neutron drip line*. If a nucleus reaches the neutron drip line, it will very quickly decay back by emitting a neutron or proton.

When equilibrium occurs, the most stable isotope will have a lower probability, usually

called *cross-section*, of neutron capture or photodisintegration. This means that these isotopes will have a relatively high abundance, as they are unlikely to undergo neutron capture or photodisintegrate. At the same time, their higher abundance will cause them to have a greater rate of β-decay than other isotopes in the isotope chain. The equilibrium is maintained until β-decay occurs, which transfers a nucleus from one isotope chain to one of a higher atomic number, forming the r-process path [2]. These processes are shown in Figure 2, which shows a general path of the r-process, with $(n, \gamma) \rightleftharpoons (\gamma, n)$ equilibrium in the isotope chains.

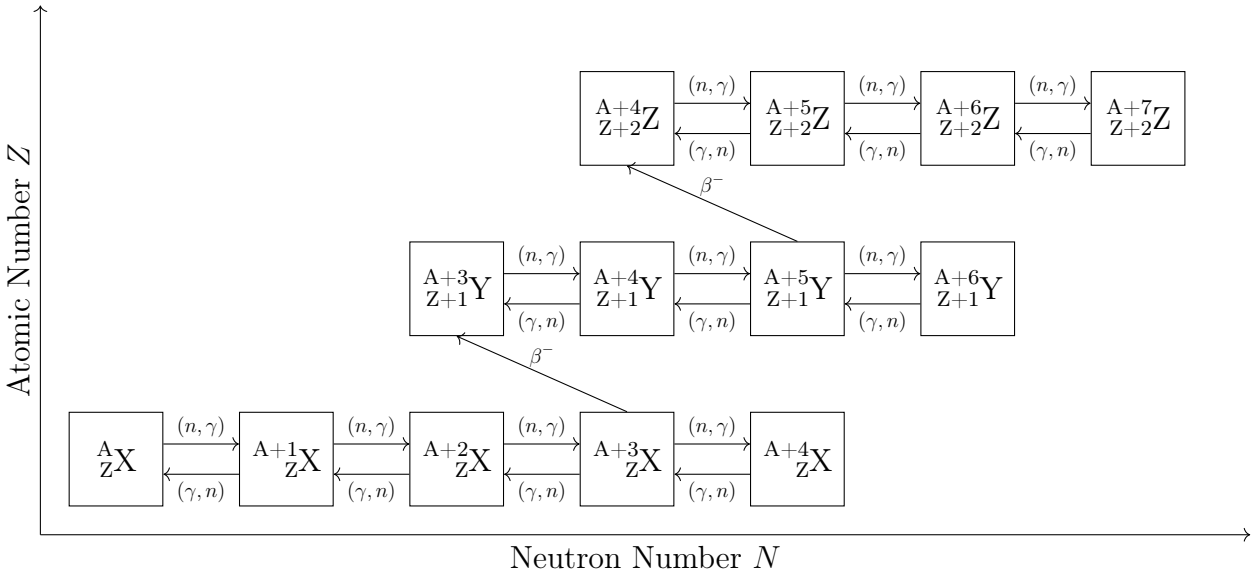

Figure 2: Neutron capture-photodisintegration equilibrium in multiple isotope chains of atomic numbers, Z, $Z + 1$ and $Z + 2$, shown in the NZ-plane. Neutron capture, (n, γ), moves the nucleus to the right in the N-direction, while photodisintegration, (γ, n), moves the nucleus to the left in the N-direction. Beta-decay, β^-, moves the nucleus from one isotope diagonally upwards and left in the NZ-plane, to a new isotope chain. These processes collectively form the r-process path.

The high neutron flux associated with r-process environments is transient. The neutron flux depends on the mass density, ρ, of the matter where the r-process occurs [16]. When ρ decreases because of expansion of the matter, the neutron flux will decrease as well. As the neutron flux decreases, the amount of neutron capture decreases and the nuclei undergo β-decay instead. Over a long time, the nuclei will decay to stable isotopes, which mark the *final abundance* of the r-process.

1.1.3 Astrophysical Sites of r-process

Some of the most poorly understood aspects of the r-process are the sites in the universe at which it takes place, and which sites are the most important for the formation of r-process elements. *Neutrino driven winds* (NDWs) were for many years believed to be the main site of the r-process [2]. Following a supernova, in which a star explodes and leaves behind a neutron star, the extremely dense neutron star is believed to cool down by emitting a large amount of neutrinos. These neutrinos may interact with matter, and may cause neutron-rich matter in the neutron star to be ejected. These neutron-rich winds will then provide a possible environment for the r-process to take place, as the neutrino driven winds collide and interact with the nuclei from the supernova. However, new research has shown that NDWs are unlikely to be the main r-process site, but it may still be the site of a *weak r-process*, in which elements with masses up to $A \sim 125$ are created [2].

One of the most plausible main r-process sites is the ejected matter from *binary neutron star mergers* (BNSMs). During a BNSM, tidal forces can cause neutron-rich matter to be ejected from the neutron stars, and additional ejecta can be produced at the contact point between the two neutron stars [2]. The neutron-rich matter is believed to be a prime candidate for the r-process sites, because of its ability to create even the heaviest r-process element, uranium [4]. Observational data of gravitational waves from Advanced Laser Interferometer Gravitational-wave Observatory (LIGO) and Virgo, together with electromagnetic observations from BNSMs have confirmed that BNSMs are a source of heavy r-process elements [4, 3, 17].

1.2 Simulation Code

The nucleosynthesis code r-Java can be used to run r-process simulations [18, 19]. The r-process simulations can be run using a full network simulation, or a *waiting-point approximation* (WPA). WPA approximates the system to be in $(n, \gamma) \rightleftharpoons (\gamma, n)$ equilibrium. This is a plausible assumption at sufficiently high temperatures and neutron densities, as

the rate of β-decay is much slower than that of neutron capture and photodisintegration. For this reason, WPA can only be run with temperatures $T \geq 2 \times 10^9$ K and neutron densities $n_n \geq 1 \times 10^{20}$ cm^{-3}. The temperature notation $T_9 = 2$ is equivalent to $T = 2 \times 10^9$ K, and will be used throughout this paper. The WPA relies only on the temperature, the neutron density n_n, and the neutron separation energy S_n, which is the amount of energy needed to remove a neutron from the nucleus [19]. The WPA lowers the computational demands and greatly decreases the simulation time, while maintaining, for the purposes of this study, sufficiently accurate results.

1.3 Previous studies

During the r-process, very neutron-rich isotopes of heavy elements are created. Because these isotopes are very unstable, there are very strict limitations on the ability to measure their properties experimentally. As new facilities for measuring the nuclear properties of very neutron-rich nuclei are constructed [20, 21], however, it is important to know which isotope measurements should be prioritised.

Previous studies have used simulations to examine the effect of individual nuclear masses, as well as the effect of other individual nuclear properties, such as β-decay rate [22, 23]. These studies found that many Sn-isotopes, as well as other isotopes, are important for the final abundance of the r-process. The most important isotopes generally have, or are close to, a *closed shell structure*, which means that their nucleus has a particularly stable structure. A closed shell occurs when either the Z or N of a nucleus has a value of 2, 8, 20, 28, 50, 82 or 126 [24]. Given that Sn has 50 protons, all Sn-isotopes have a closed shell structure, making them especially stable, which may contribute to their importance in the r-process. The studies have analysed a great number of isotopes, but have not, however, examined the heaviest Sn-isotopes, close to the neutron drip line [22, 23].

In these studies, the *F-value*, which is calculated as

$$F = 100 \sum_A |X_{baseline}(A) - X_{\Delta m}(A)| \tag{4}$$

is used as a measure of difference between r-processes with different nuclear masses [22, 23]. The mass fraction $X(A)$ is the fraction of the total mass that is attributed to nuclei with atomic mass number A. This compares the mass fraction, $X_{baseline}(A)$, in a simulation with nuclear masses in accordance with the used mass models, with the mass fraction, $X_{\Delta m}(A)$, in a simulation with adjusted nuclear masses.

1.4 Aim of Study

This study aims to determine which r-process environment, with regard to initial temperature and mass density, is most sensitive to the masses of Sn-isotopes, specifically those with atomic mass numbers between $A = 146$ and $A = 166$. This is done by simulating the r-process using r-Java and varying the initial temperature and density, and comparing the final abundances of the r-process with and without varied masses of the Sn-isotopes.

Furthermore, this study will examine which individual Sn-isotope masses are most critical for the final abundance in the most sensitive environment. This is done by simulating the r-process and determining the impact of Sn-isotopes by varying a single Sn-isotope mass for each simulation.

2 Method

Using r-Java, r-process WPA simulations were run to quantify the difference that the masses of Sn-isotopes, with atomic mass numbers between $A = 146$ and $A = 166$, have on the final abundance of the r-process. The differences between simulations were calculated as F-values using Equation (4). For all simulations, an electron fraction, $Y_e = 0.15$ was used. The electron fraction can also be described as the ratio of the number of protons to the total number of nucleons, Z/A. Thus, a lower value of Y_e means that the matter is more neutron-rich. The value of $Y_e = 0.15$ was used as it is within the commonly predicted Y_e-values for BNSMs, as well as for NDWs [2]. Furthermore, all simulations assumed that the seed nuclei consisted entirely of ^{90}Se [25].

2.1 Temperature and Density Variations

Simulations to quantify the sensitivity to Sn-isotope masses in different environments were run by varying the initial temperatures and densities of the simulations. Simulations were run for three different initial temperatures, $T_9 = 2$, $T_9 = 3$ and $T_9 = 4$, and six different initial densities $\rho_0 = 1 \times 10^7\,\mathrm{g\,cm^{-3}}$, $\rho_0 = 1 \times 10^8\,\mathrm{g\,cm^{-3}}$, $\rho_0 = 1 \times 10^9\,\mathrm{g\,cm^{-3}}$, $\rho_0 = 1 \times 10^{10}\,\mathrm{g\,cm^{-3}}$, and $\rho_0 = 1 \times 10^{11}\,\mathrm{g\,cm^{-3}}$. For a given temperature and density, a baseline simulation was run using the Hartree-Fock-Bogoliubov 21 mass model (HFB-21), which is a mass model for predicting nuclear masses near the neutron drip line [26, 27, 28]. Another simulation, using HFB-21, but with masses increased by 20 MeV for all Sn-isotopes between $A = 146$ and $A = 166$. The mass change is given in MeV because a changed mass affects the energy with which particles in the nucleus are bound. The impact of the changed masses was quantified using the F-value.

2.2 Mass Variations

For the temperature and density of highest sensitivity to the Sn isotope masses, additional simulations were run. The mass of a single Sn-isotope between $A = 146$ and $A = 166$ was increased by 20 MeV for each simulation. Thus, the impact of the mass of each Sn-isotope could be quantified by the F-value. For the baseline simulation HFB-21 was used, and the simulations with mass variations used HFB-21 with individual isotope masses increased by 20 MeV.

3 Results

This section covers the results from the simulations. First, the results from simulations with varied initial temperatures and densities are presented. Second, the results from the simulations with individually varied isotope masses will be presented.

3.1 Temperature and Density Variations

The results indicate that using an initial temperature $T_9 = 2$ and density $\rho_0 = 1 \times 10^{10}\,\mathrm{g\,cm^{-3}}$ created the environment most sensitive to variations in the Sn-isotope masses. As shown in Figure 3, only 9 environments yielded results, as the numerical methods of r-Java could not compute results for all initial temperatures and densities. A full table of the F-value for each environment is provided in Appendix A.

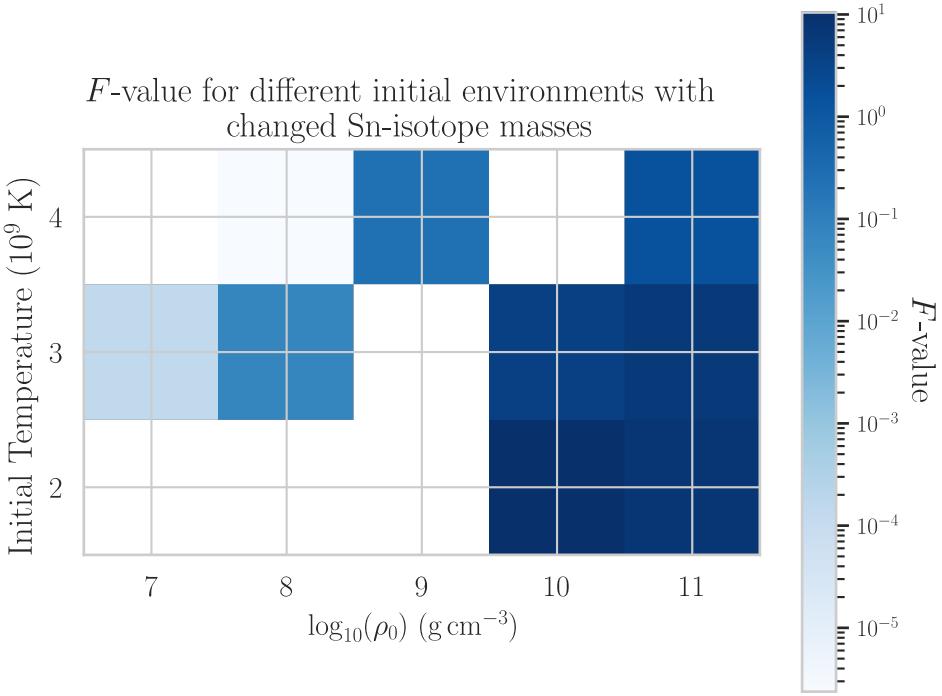

Figure 3: Using 15 different initial temperature and density configurations, the impact of nuclear masses for Sn-isotopes with atomic mass numbers between $A = 146$ and $A = 166$ was quantified by simulating the r-process. Only 9 simulations yielded results, as r-Java could not compute results for all environments. For each environment, the F-value, which is the difference in final abundance between the baseline case and the case with changed masses, is shown.

3.2 Mass Variations

The results of the mass variation simulations indicate that a mass increase of 20 MeV has a large impact on the final abundance of the r-process, for a lot of Sn-isotopes heavier than $A = 146$. Figure 4 shows the F-value of each isotope when its mass has been increased.

There are some isotopes, such as ^{142}Sn and ^{163}Sn for which the F-value is significantly

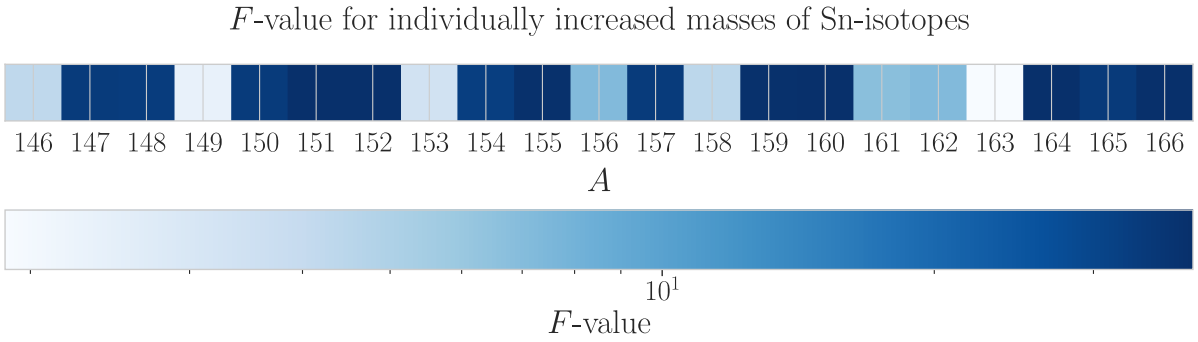

Figure 4: For an initial temperature $T_9 = 2$ and density $\rho_0 = 1 \times 10^{10}\,\mathrm{g\,cm^{-3}}$, simulations were run for 21 different mass configurations and compared with a baseline case. By increasing the mass of one isotope for each simulation by 20 MeV, the final abundances could be compared with the baseline case. The figure shows the F-value for each isotope, indicating the size of the difference to the baseline case.

smaller than others. Similarly, there are a few isotopes for which the F-value is very high, such as ^{152}Sn, ^{160}Sn, and ^{166}Sn. A full table of F-values for each isotope is provided in Appendix B.

4 Discussion

The results demonstrate the impact of both nuclear and astrophysical conditions during the r-process. While both these factors remain largely uncertain, new discoveries may improve the understanding of the r-process. The new LIGO and VIRGO observational data, together with electromagnetic observations [17, 3], may improve the understanding of the astrophysical conditions of BNSMs, which is believed to be the one of the most plausible r-process sites. Furthermore, new facilities such as Facility for Rare Isotope Beams at Michigan State University and Facility for Antiproton and Ion Research in Darmstadt, Germany will be able to provide new observations of nuclear properties [20, 21], which will facilitate the formulation of improved mass models and r-process simulations.

4.1 Temperature and Density Variations

Though only 9 of the 15 simulations pertaining to temperature and density variations yielded results, the results indicate that a lower temperature of $T_9 = 2$ is more sensitive to the masses of the Sn-isotopes, as the F-value in Figure 3 increases with decreasing temperature. Though this should not be considered a general correlation, it may have a physical explanation. As the temperature increases, the (γ, n)-photodisintegration rate should also increase, due to higher amounts of γ-rays being emitted at higher temperatures. Higher photodisintregration rates may cause the r-process path to remain further from the neutron drip line, which would also cause the Sn-isotopes to have a smaller effect on the r-process.

Similarly, because the neutron flux depends on the mass density, a higher initial mass density, ρ_0, will result in a higher neutron flux. A higher neutron flux will increase the amount of neutron capture, bringing the r-process path closer to the neutron drip line. Therefore, an environment with higher initial density should be more sensitive to the mass of the Sn-isotopes, though this is contradicted by the results for $T_9 = 2$ as shown in Figure 3. This is attributed to the fact that a temperature of $T_9 = 2$ and initial density $\rho_0 = 1 \times 10^{10}\,\mathrm{g\,cm^{-3}}$ creates an r-process path that is "pushed" toward the neutron drip line, such that the lightest Sn-isotopes with changed masses do not impact the r-process as much.

To summarise, the F-value distribution shown in Figure 3 could be explained by taking into consideration the factors that can affect the r-process path.

4.2 Mass Variations

From the simulations pertaining to mass variations, it is evident that different isotopes seem to play a very different role in the r-process. Of the 21 isotopes whose masses were changed, 13 had an F-value above 30. The mass increase of 20 MeV can be considered large, and similar studies have used significantly smaller mass changes [23]. We may,

however, conclude that some isotopes have a significantly larger impact on the r-process than others, and may thus be considered as more important to study experimentally. The nuclei of ^{151}Sn, ^{152}Sn, ^{155}Sn, ^{159}Sn, ^{160}Sn, ^{164}Sn, and ^{166}Sn all had F-values greater than 38. However, the F-values should, to an unknown extent, have been affected by the environment, and comparisons among the isotopes may be specific to the simulated temperatures and densities.

4.3 Further Research

Future studies should take into consideration the astrophysical candidates, such as BNSMs and NDWs, to find simulation parameters that reflect the understanding of the astrophysical environment during the r-process. This could yield more conclusive results as to what isotopes are important to measure to improve both the understanding and simulations of the r-process as a whole. Such understanding and simulations could also provide a conclusive answer as to which potential r-process site is the most important. Simulating the individual mass changes in many different environments could also provide more general results regarding the importance of different isotopes.

Furthermore, more accurate results could be obtained by including other properties in the mass changes. As the mass is increased or decreased, the β-decay rates, neutron capture rates, and photodisintegration rates should also be affected. Estimations of these changes based on the changed masses could provide further improvements upon the results.

4.4 Conclusion

This study has identified that the importance of nuclear masses for specific nuclei depends on the environment in which the r-process occurs. The results indicated that an initial temperature $T_9 = 2$ and initial mass density $\rho_0 = 1 \times 10^{10}\,\mathrm{g\,cm^{-3}}$ created an r-process environment in which heavy Sn-isotopes have a large effect on the final abundance. This

study also compared the effect of individual Sn-isotope masses in this environment on the final abundance. These results demonstrated that there is a large difference among different isotopes in their importance for the r-process abundances.

These results are important as new technology enables us to experimentally measure the properties of further heavier nuclei. Primarily, however, further research should continue this search of critical nuclei, by comparing the impact of the individual isotopes in different astrophysical environments.

References

[1] Arnould M, Goriely S, Takahashi K. The r-process of stellar nucleosynthesis: Astrophysics and nuclear physics achievements and mysteries. Physics Reports. 2007;450(4):97-213. Available from: https://www.sciencedirect.com/science/article/pii/S0370157307002438.

[2] Kajino T, Aoki W, Balantekin AB, Diehl R, Famiano MA, Mathews GJ. Current status of r-process nucleosynthesis. Progress in Particle and Nuclear Physics. 2019;107:109-66. Available from: https://www.sciencedirect.com/science/article/pii/S0146641019300201.

[3] Chen MH, Li LX, Lin DB, Liang EW. Gamma-Ray Emission Produced by r-process Elements from Neutron Star Mergers. The Astrophysical Journal. 2021;919(1):59.

[4] Horowitz CJ, Arcones A, Côté B, Dillmann I, Nazarewicz W, Roederer IU, et al. r-process nucleosynthesis: connecting rare-isotope beam facilities with the cosmos. Journal of Physics G: Nuclear and Particle Physics. 2019 jul;46(8):083001. Available from: https://doi.org/10.1088/1361-6471/ab0849.

[5] Alpher RA, Bethe H, Gamow G. The Origin of Chemical Elements. Phys Rev. 1948 Apr;73:803-4. Available from: https://link.aps.org/doi/10.1103/PhysRev.73.803.

[6] Cyburt RH, Fields BD, Olive KA, Yeh TH. Big bang nucleosynthesis: Present status. Reviews of Modern Physics. 2016 feb;88(1). Available from: https://doi.org/10.1103%2Frevmodphys.88.015004.

[7] Brorsson J, Jacobsson J, Johansson A. Big Bang Nucleosynthesis [B.S. thesis]; 2010.

[8] Steigman G. Big Bang Nucleosynthesis: Probing the First 20 Minutes. arXiv; 2003. Available from: https://arxiv.org/abs/astro-ph/0307244.

[9] Ryden B. Introduction to cosmology. Cambridge University Press; 2017.

[10] Ström E. Big Bang nucleosynthesis with a historical touch; 2021.

[11] Bromm V, Yoshida N, Hernquist L, McKee CF. The formation of the first stars and galaxies. Nature. 2009;459(7243):49-54.

[12] Arnould M, Takahashi K. Nuclear astrophysics. Reports on Progress in Physics. 1999;62(3):395.

[13] Reifarth R. The s-process – overview and selected developments. Journal of Physics: Conference Series. 2010 jan;202:012022. Available from: https://doi.org/10.1088/1742-6596/202/1/012022.

[14] Cowan JJ, Thielemann FK. R-Process Nucleosynthesis in Supernovae. Physics Today. 2004;57(10):47-53. Available from: https://doi.org/10.1063/1.1825268.

[15] Möller P, Pfeiffer B, Kratz KL. New calculations of gross β-decay properties for astrophysical applications: Speeding-up the classical r process. Physical Review C. 2003;67(5):055802.

[16] Freiburghaus C, Rosswog S, Thielemann FK. R-process in neutron star mergers. The Astrophysical Journal. 1999;525(2):L121.

[17] Chornock R, Berger E, Kasen D, Cowperthwaite P, Nicholl M, Villar V, et al. The electromagnetic counterpart of the binary neutron star merger LIGO/VIRGO GW170817. IV. Detection of near-infrared signatures of r-process nucleosynthesis with Gemini-south. The Astrophysical Journal Letters. 2017;848(2):L19.

[18] Kostka M, Koning N, Shand Z, Ouyed R, Jaikumar P. r-Java 2.0: the astrophysics. arXiv preprint arXiv:14023824. 2014.

[19] Kostka M, Koning N, Shand Z, Ouyed R, Jaikumar P. The r-Java 2.0 code: nuclear physics. Astronomy & Astrophysics. 2014;568:A97.

[20] Motobayashi T. World new facilities for radioactive isotope beams. In: EPJ Web of Conferences. vol. 66. EDP Sciences; 2014. p. 01013.

[21] Ostroumov P, Hausmann M, Fukushima K, Maruta T, Plastun A, Portillo M, et al. Heavy ion beam physics at Facility for Rare Isotope Beams. Journal of Instrumentation. 2020;15(12):P12034.

[22] Brett S, Bentley I, Paul N, Surman R, Aprahamian A. Sensitivity of the r-process to nuclear masses. The European Physical Journal A. 2012;48(12):1-5.

[23] Mumpower MR, Surman R, McLaughlin G, Aprahamian A. The impact of individual nuclear properties on r-process nucleosynthesis. Progress in Particle and Nuclear Physics. 2016;86:86-126.

[24] Heyde KL. The nuclear shell model. In: The Nuclear Shell Model. Springer; 1994. p. 58-154.

[25] Qian YZ, Vogel P, Wasserburg G. Diverse supernova sources for the r-process. The Astrophysical Journal. 1998;494(1):285.

[26] Samyn M, Goriely S, Heenen PH, Pearson J, Tondeur F. A hartree–fock–bogoliubov mass formula. Nuclear Physics A. 2002;700(1-2):142-56.

[27] Goriely S, Hilaire S, Koning AJ. Improved predictions of nuclear reaction rates with the TALYS reaction code for astrophysical applications. Astronomy & Astrophysics. 2008;487(2):767-74.

[28] Goriely S, Chamel N, Pearson J. Further explorations of Skyrme-Hartree-Fock-Bogoliubov mass formulas. XII. Stiffness and stability of neutron-star matter. Physical Review C. 2010;82(3):035804.

A *F*-values for Temperature and Density Variations

Table 1: The F-value for different initial environments when the masses of Sn-isotopes with atomic mass numbers between $A = 146$ and $A = 166$ were increased by 20 MeV. The final abundances were compared to a simuation with the same initial parameters, but with no masses changed.

ρ_0 ($\mathrm{g\,cm^{-3}}$)	T (10^9 K)	F-value
1×10^7	2	NaN
1×10^7	3	0.0001322
1×10^7	4	NaN
1×10^8	2	NaN
1×10^8	3	0.06671
1×10^8	4	0.000002377
1×10^9	2	NaN
1×10^9	3	NaN
1×10^9	4	0.2397
1×10^{10}	2	10.45
1×10^{10}	3	3992
1×10^{10}	4	NaN
1×10^{11}	2	7.142
1×10^{11}	3	5.990
1×10^{11}	4	1.463

B *F*-values for Mass Variations

Table 2: The F-value for each isotope as its mass was increased by 20 MeV. The simulations were run with initial parameters $T_9 = 2$ and $\rho_0 = 1 \times 10^{10}\,\mathrm{g\,cm^{-3}}$, and compared to a baseline simulation with no changed masses. The F-value was calculated using Equation (4).

Nucleus	F-value
^{146}Sn	4.279
^{147}Sn	33.93
^{148}Sn	33.48
^{149}Sn	2.373
^{150}Sn	33.70
^{151}Sn	38.28
^{152}Sn	38.53
^{153}Sn	3.377
^{154}Sn	32.60
^{155}Sn	38.13
^{156}Sn	7.139
^{157}Sn	33.76
^{158}Sn	4.370
^{159}Sn	38.13
^{160}Sn	38.36
^{161}Sn	6.743
^{162}Sn	7.214
^{163}Sn	1.875
^{164}Sn	38.20
^{165}Sn	34.01
^{166}Sn	38.65